ACCOUNTS of chemical research

Hydrogen Evolution Catalyzed by Cobaloximes

JILLIAN L. DEMPSEY, BRUCE S. BRUNSCHWIG,*
JAY R. WINKLER,* AND HARRY B. GRAY*
Beckman Institute, California Institute of Technology, Pasadena, California 91125

RECEIVED ON SEPTEMBER 30, 2009

CONSPECTUS

Natural photosynthesis uses sunlight to drive the conversion of energy-poor molecules (H_2O, CO_2) to energy-rich ones (O_2, $(CH_2O)_n$). Scientists are working hard to develop efficient artificial photosynthetic systems toward the "Holy Grail" of solar-driven water splitting. High on the list of challenges is the discovery of molecules that efficiently catalyze the reduction of protons to H_2. In this Account, we report on one promising class of molecules: cobalt complexes with diglyoxime ligands (cobaloximes).

Chemical, electrochemical, and photochemical methods all have been utilized to explore proton reduction catalysis by cobaloxime complexes. Reduction of a Co^{II}-diglyoxime generates a Co^{I} species that reacts with a proton source to produce a Co^{III}-hydride. Then, in a homolytic pathway, two Co^{III}-hydrides react in a bimolecular step to eliminate H_2. Alternatively, in a heterolytic pathway, protonation of the Co^{III}-hydride produces H_2 and Co^{III}.

A thermodynamic analysis of H_2 evolution pathways sheds new light on the barriers and driving forces of the elementary reaction steps involved in proton reduction by Co^{I}-diglyoximes. In combination with experimental results, this analysis shows that the barriers to H_2 evolution along the heterolytic pathway are, in most cases, substantially greater than those of the homolytic route. In particular, a formidable barrier is associated with Co^{III}-diglyoxime formation along the heterolytic pathway.

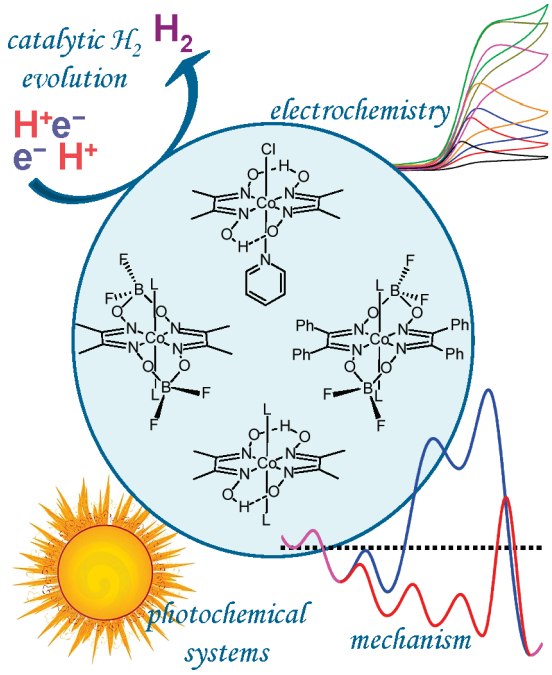

Our investigations of cobaloxime-catalyzed H_2 evolution, coupled with the thermodynamic preference for a homolytic route, suggest that the rate-limiting step is associated with formation of the hydride. An efficient water splitting device may require the tethering of catalysts to an electrode surface in a fashion that does not inhibit association of Co^{III}-hydrides.

Introduction

In response to the current global energy crisis, scientists are going to great lengths to develop renewable resources capable of meeting projected energy demands.[1,2] Solar energy conversion is an area of enormous promise; using sunlight to make "solar fuels" such as H_2 (from H_2O splitting, Figure 1) and CH_3OH (by reducing CO_2) is one of the Holy Grails of 21st century chemistry.[3,4] Splitting water is highly desirable, because 4.92 eV is stored when two H_2O molecules are split into two H_2 and O_2, but running the reaction is challenging; it involves two separate multielectron redox processes, a four-electron oxidation and a two-electron reduction.[5] Because sequential electron or hole transfers directly to H_2O produce extremely high-energy intermediates, an energy-efficient process requires catalysts that avoid formation of these species.[6,7] Coordination to metals in some cases can stabilize these energetic inter-

Published on the Web 11/23/2009 www.pubs.acs.org/acr
10.1021/ar900253e

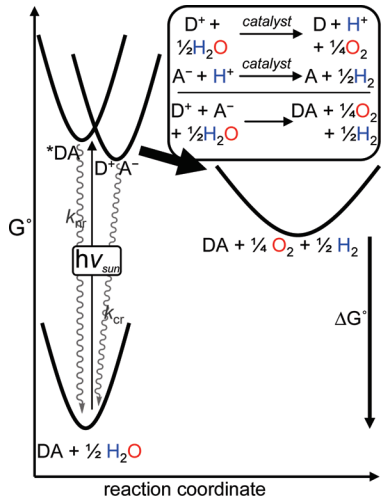

FIGURE 1. Solar energy conversion is initiated by photoexcitation ($h\nu_{sun}$) of DA to *DA, which undergoes excited-state electron transfer to yield a charge-separated state (D^+A^-). D^+ and A^- drive water oxidation and proton reduction via catalysts.

mediates, thereby lowering the barriers for hydrogen evolution.[8] One of the best catalysts is platinum, which operates at the thermodynamic potential for H^+/H_2 conversion (0 V vs SHE, pH 0).[9] Notable among other highly active catatlysts are [FeFe], [NiFe], and [Fe] hydrogenases,[10−21] which have inspired a great deal of work on synthetic metallobiomolecules aimed at mimicking proton reduction and H_2 oxidation functionalities.[22−31]

Although the ultimate objective is to use water as a feedstock,[32−38] many potential H_2 evolving catalysts are tested for catalytic activity in organic solvents, because they often are not soluble or stable in aqueous environments. The electrocatalytic behavior of proton sources in organic solvents is markedly different from that in aqueous environments. In nonaqueous solvents, the standard potential for hydrogen evolution, E°_{HA/H_2}, is directly related to acid strength, and can be described by

$$E^\circ_{HA/H_2} = E^\circ_{HA/H_2} - (2.303RT/F)pK_{a,HA}$$

where $E^\circ_{H^+/H_2}$ is the solvated proton/dihydrogen couple standard potential in the given solvent and $K_{a,HA}$ is the acid dissociation constant for the proton source.[39] The standard potentials for hydrogen evolution from a variety of commonly used acids is given in Table 1. The overpotential for proton reduction, is the difference between the potential of catalytic activity and E°_{HA/H_2}; we do not expect to achieve catalysis at potentials more positive than E°_{HA/H_2}.

Metal complexes that catalyze the reduction of protons to H_2 in organic solvents[40−43] include $(CpMo\mu\text{-}S)_2S_2CH_2$,[44] which operates at −0.26 V vs SCE in CH_3CN with (*p*-cyanoanilinium)-BF_4 as a proton source, and $[Ni(P^{Ph}_2N^{Ph}_2)_2(CH_3CN)]^{2+}$, which is active at −0.46 V vs SCE with trifluoromethanesulfonic acid.[45] Cobalt complexes with diglyoxime ligands (Figure 2) also have been shown to catalyze hydrogen evolution at low overpotentials; the proton reduction chemistry of these catalysts will be highlighted in this Account.

TABLE 1. pK_a Values and Standard Potentials for Reduction of Acids in Acetonitrile

acid	pK_a[a]	E°_{HA/H_2} (V vs SCE)[c]
$HBF_4 \cdot Et_2O$	0.1[b]	0.23
trifluoromethanesulfonic acid	2.6	0.09
p-cyanoanilnium	7.6	−0.21
$TsOH \cdot H_2O$	8.0[b]	−0.23
$HCl \cdot Et_2O$	8.9[b]	−0.29
CF_3COOH	12.7[b]	−0.51
$[Et_3NH]^+$	18.7	−0.86
$[Et_3NH]^+$	9.2 (DMF)	−0.84
acetic acid	13.2 (DMF)	−1.08

[a] Reference 39 unless noted otherwise. [b] Reference 81. [c] $E^\circ_{HA/H_2} = E^\circ_{H^+/H_2} - 0.059pK_a(HA)$. A potential of 0.24 V vs SCE was chosen as the thermodynamic potential for $E^\circ_{H^+/H_2}$ in acetonitrile (ref 50).

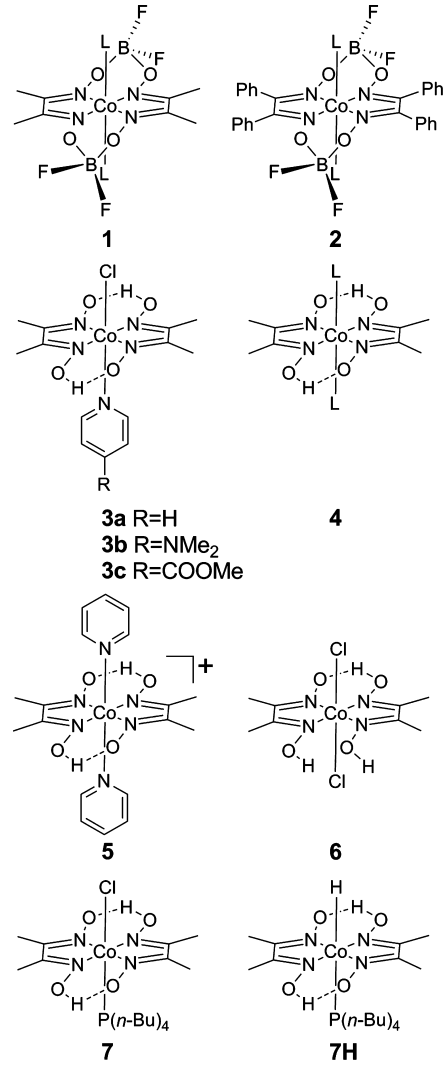

FIGURE 2. Cobaloxime complexes. L is typically H_2O or CH_3CN.

TABLE 2. Electrochemical Potentials (V vs SCE in Acetonitrile)

complex	$E°(Co^{III/II})$	$E°(Co^{II/I})$	ref
1	∼0.2[a]	−0.55	48
2	∼0.3[a]	−0.28	48
3a	−0.68	−1.13	59[b]
3b	−0.84	−1.13	59[b]
3c	−0.78	−1.09	59[b]
5	−0.39	−1.1	59[b]
6	−0.49	−0.8	59[b]
7	−0.92	−0.99	59[b]

[a] Irreversible couple. [b] NHE vs SCE = −0.25 V in acetonitrile (ref 82).

Electrochemical Systems

Connolly and Espenson first reported that $Co(dmgBF_2)_2(L)_2$ (**1**, $dmgBF_2$ = difluoroboryl-dimethylglyoxime) catalyzes the reduction of HCl_{aq} using $Cr^{2+}{}_{aq}$ as a stoichiometric electron donor.[46] Dissociation of an intermediate chloro-bridged complex, $[(H_2O)_5Cr{-}Cl{-}Co(dmgBF_2)_2]^+$, which was formed during inner-sphere electron transfer from Cr^{II} to Co^{II}, produces $[Co(dmgBF_2)_2L]^-$ ($\mathbf{1}^-$). In the presence of acid, it is likely that the Co^I anion is rapidly protonated to form a hydride, $[HCo(dmgBF_2)_2L]$, which evolves H_2.

Complex **1** and a related species, $Co(dpgBF_2)_2(L)_2$ (**2**, dpg = difluoroboryl-diphenylglyoxime),[47] were later shown electrochemically to catalyze H_2 evolution in CH_3CN.[48,49] The reversible, one-electron reduction of **1** occurs at −0.55 V vs SCE in CH_3CN (Table 2). Upon addition of a sufficiently strong acid, catalytic currents were observed near the $Co^{II/I}$ couple. Increasing acid concentration produced an increase in peak current, a slight positive shift in peak position, and loss of the return oxidation wave, with the current eventually approaching a plateau. Since Co^{II} is regenerated during H_2 production, there is no return oxidation wave. Bulk electrolysis experiments confirmed near quantitative Faradaic yields of H_2. A range of proton sources was examined: catalysis was observed with CF_3COOH, $HCl \cdot Et_2O$, *p*-toluenesulfonic acid monohydrate ($TsOH \cdot H_2O$),[50] (*p*-cyanoanilinium)BF_4, and $HBF_4 \cdot Et_2O$. Although $HBF_4 \cdot Et_2O$ was shown to effect H_2 evolution with substantially increased rates, competitive degradation pathways of the catalyst greatly limited reaction efficiencies.

Substitution of methyl groups by electron-withdrawing phenyl substituents to form **2** shifts the $Co^{II/I}$ reduction potential 270 mV positive to −0.28 V vs SCE. Electrocatalysis was observed with $HCl \cdot Et_2O$, (*p*-cyanoanilinium)BF_4, $TsOH \cdot H_2O$, and $HBF_4 \cdot Et_2O$, but *not* CF_3COOH, with currents reaching a plateau at high acid concentrations.

Studies of cobalt difluoroboryl-diglyoximes as well as related compounds with [14]-tetraene-N_4 ligands led to a correlation between catalyst activity (H_2 evolution) and $Co^{II/I}$ potentials.[50] Complexes with more negative reduction potentials were able to catalyze proton reduction with weaker acids at higher rates than those with more positive reduction potentials. Metal hydride pK_a values increase as the $Co^{II/I}$ reduction potentials become more negative; thus the $Co^{II/I}$ potentials are related to Co^I basicities.[51]

TABLE 3. Electrochemical Potentials (V vs SCE in DMF)[a]

complex	$E°(Co^{III/II})$	$E°(Co^{II/I})$	ref
3a	−0.67	−1.06	52
3b	−0.74	−1.09	52
4		−1.06	52
5	−0.32	−1.06	52
7	−0.70	−0.89	52

[a] Converted to SCE from Ag/AgCl/3 mol L^{-1} NaCl, Fc^+/Fc vs Ag/AgCl = 0.55 V in DMF (ref 52), Fc^+/Fc vs SCE = 0.47 V in DMF (ref 83).

The overpotentials for proton reduction catalyzed by cobaloxime complexes can be estimated from the difference between $E°_{HA/H_2}$ and the potential where catalytic behavior is observed, which occurs just negative of $E°(Co^{II/I})$. Catalysts that reduce protons near the thermodynamic potential also should oxidize H_2 in the presence of a conjugate base. Indeed, slow oxidation of H_2 by **1** in the presence of $[NBu_4]CF_3CO_2$ has been observed. The H_2 evolution overpotential was calculated to be 90 mV based on the reaction equilibrium constant.[50]

The electrocatalytic behavior of similar cobalt diglyoximes also has been examined. $Co(dmgH)_2pyCl$ (**3a**, py = pyridine) catalyzes H_2 evolution at a $Co^{II/I}$ potential of −1.06 V vs SCE in DMF with $[Et_3NH^+]Cl$ (Table 3).[52] Upon reduction to the Co^{II} species, the halide ligand is labilized, while the axial pyridine stays coordinated. Substitution of the axial pyridine for 4-(dimethylamino)pyridine (**3b**) does not substantially modify the $Co^{II/I}$ potential, but the catalyst appears to be more electroactive.

$Co(dmgH)_2L_2$ (**4**) has the same $Co^{II/I}$ reduction potential as **3** in DMF.[52] The glyoxime bridging BF_2 groups, produced via reaction of the complex with $BF_3 \cdot Et_2O$,[53] shift $Co^{II/I}$ potentials to values ∼0.5 V more positive than their corresponding hydrogen-bridged counterparts but require stronger acids for electrocatalytic hydrogen evolution. The bridging BF_2 groups also increase the stability of the catalysts in acidic solutions.

Photochemical Systems

Catalytic hydrogen production can be driven directly with light when a sacrificial electron donor is present to scavenge the oxidized photosensitizer.[54,55] Photosensitizers can act as both light harvesters and photoreductants; quenching their electronic excited states by electron transfer, directly to a catalyst or via an electron mediator, generates the reduced catalyst. Zeissel and co-workers demonstrated a multicomponent photochemical system for homogeneous H_2 generation with a cobaloxime catalyst in organic solvents, utilizing

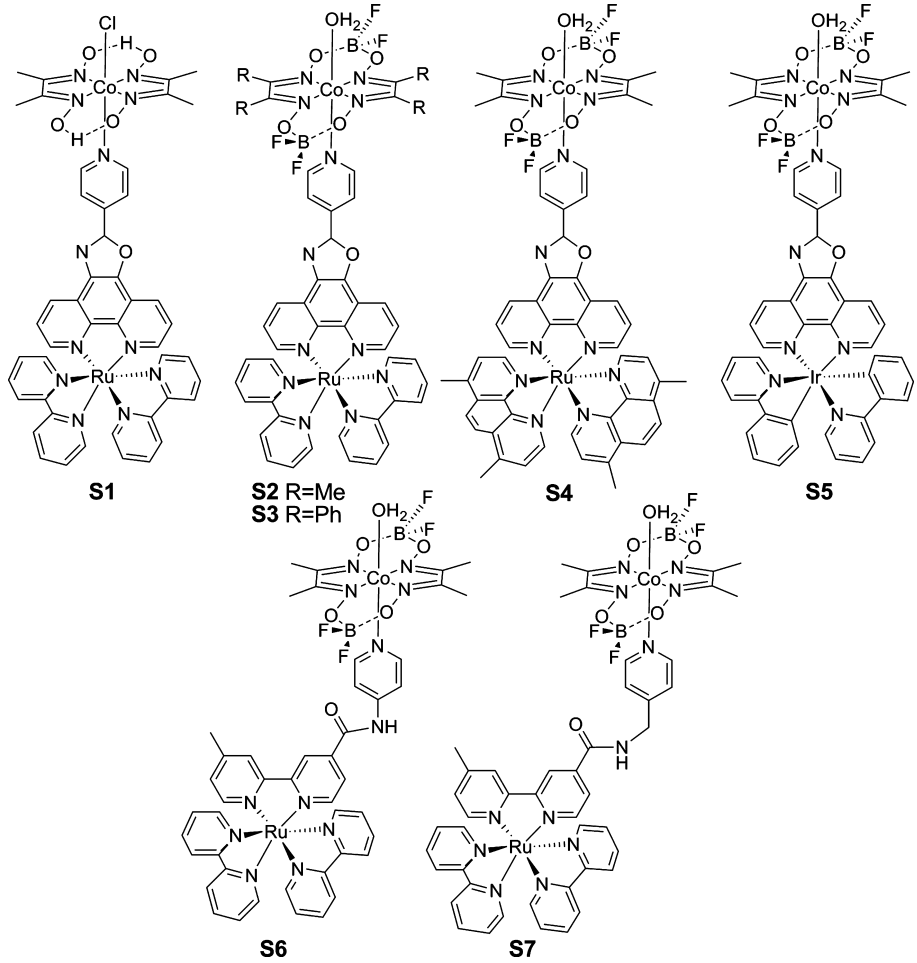

FIGURE 3. Sensitizer−cobaloxime conjugates for photocatalytic hydrogen evolution.

$[Ru(bpy)_3]^{2+}$ (bpy = 2,2′-bipyridine) as photosensitizer, triethanolamine (TEOA) as sacrificial electron donor, and **4** as catalyst.[56] In DMF solution at pH 8.8, the turnover number for 1 h of irradiation (based on photosensitizer concentration) was 38.

Among other work of note,[57] Eisenberg and co-workers have shown that **3a** catalyzes H_2 evolution with a platinum(II) terpyridyl phenylacetylide complex, $[Pt(ttpy)(C{\equiv}CPh)]^+$ (ttpy = 4′-*p*-tolylterpyridine), as photosensitizer and TEOA as a donor in 3:2 (v/v) CH_3CN/H_2O solutions between pH 7 and pH 12.[58] At pH 8.5 with 0.27 M TEOA, 1000 turnovers were achieved after 10 h irradiation ($\lambda > 410$ nm).

Other cobaloxime catalysts with varying axial bases (**3a**−**c**, **5**−**7**) and Pt(II) acetylide photosensitizers have been investigated.[59] With **3a** as catalyst, 2150 turnovers of H_2 were achieved after 10 h irradiation ($\lambda > 410$ nm) in a 24:1 (v/v) CH_3CN/H_2O mixture at pH 8.5. Systems also have been reported in which organic chromophores replaced noble metal photosensitizers.[60] In 12 h of irradiation ($\lambda > 450$ nm), 900 turnovers were achieved using the eosin Y photosensitizer with **3a**, TEOA, and 3 mM free dimethylglyoxime in 1:1 CH_3CN/H_2O at pH 7. Degradation of the photosensitizer/catalyst system was minimized with added dimethylglyoxime.

Fontecave and co-workers have focused on multicomponent photosystems for H_2 evolution with **1** and both $[Ir(ppy)_2(phen)]^+$ (ppy = 2-phenylpyridine, phen = phenanthroline) and $[ReBr(CO)_3(phen)]$ as photosensitizers in acetone. Solutions were buffered using Et_3N/Et_3NH^+, which provided both a sacrificial donor (Et_3N) and a proton source (Et_3NH^+).[61] A quantum yield of 16% ± 1% and 273 turnovers were achieved with $[ReBr(CO)_3(phen)]$ in a 15 h experiment ($\lambda > 380$ nm) with 600 equivalents each of Et_3N and Et_3NH^+.

Alberto and co-workers studied a similar photosystem with **4**, employing $[ReBr(CO)_3(bpy)]$ as a photosensitizer, 1 M TEOA as sacrificial electron donor, and 0.1 M acetic acid as a proton source in DMF.[62] They observed 150 turnovers in 9 h irradiation ($\lambda > 400$ nm) for the system, which had a 26% ± 2% quantum yield. Dimethylglyoxime (7.5 mM) was added to enhance catalytic activity.

Bifunctional systems (Figure 3) have been reported recently with photosensitizers coordinated directly via axial pyridine

SCHEME 1. H_2 Evolution Pathways

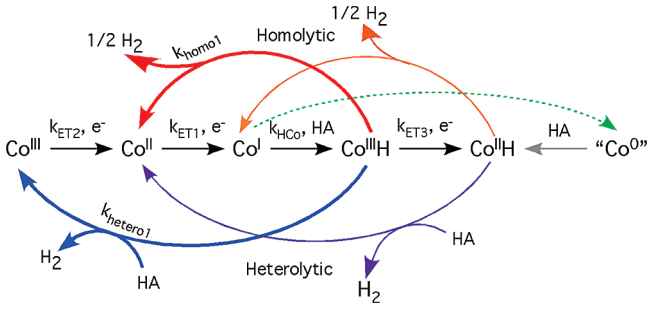

ligands to $[Co(dmgBF_2)_2(H_2O)]$ and $[Co(dmgH)_2Cl]$ (**S1**−**S5**).[61,63] Irradiation of these sensitizer−catalyst conjugates in Et_3N/Et_3NH^+ buffered acetone solution triggers intramolecular electron transfer from photoexcited ruthenium or iridium sensitizers to the cobalt center, leading to H_2 evolution. Notably, these conjugates exhibited efficiencies up to 8.5 times greater than analogous multicomponent systems under the same conditions: $[(ppy)_2Ir((L\text{-}pyr)Co(dmgBF_2)_2(H_2O)]^+$ (**S5**, L-pyr = (4-pyridine)oxazolo[4,5-f]phenanthroline) managed 210 turnovers after 15 h irradiation with 600 equivalents of Et_3N and Et_3NH^+ in acetone. Li et al. studied related heterobinuclear Ru−Co systems with (**S6**) and without (**S7**) linker conjugation.[64] While both complexes were more active than the corresponding multicomponent systems, the one with a nonconjugated bridge exhibited more turnovers.

Reaction Pathways

Pathways for proton reduction by cobalt complexes are shown in Scheme 1. Reduction to a Co^I species that can be protonated to form $Co^{III}H$ must occur first. The hydride can react in a bimolecular step with another hydride to eliminate H_2 (homolytic or bimetallic route, red pathway), or it can be protonated,[65] release H_2, and generate Co^{III} that is subsequently reduced (heterolytic or monometallic route, blue pathway). Alternatively, the $Co^{III}H$ can be reduced further to yield $Co^{II}H$,[43] which can react via an analogous homolytic (orange) or heterolytic (purple) pathway. If the Co^I species is not protonated, it can be reduced further to a "Co^0" species (which could be Co^I with a ligand radical), which, upon protonation to form $Co^{II}H$ (green pathway), can react as above.

Chao and Espenson studied the reactivity of kinetically stabilized $[HCo(dmgH)_2P(n\text{-}C_4H_9)_3]$ (**7H**) in order to ascertain the pathway of H_2 formation.[66] Interpretation of hydride reaction kinetics in the presence of acid (aqueous) required a rate expression that was both first- and second-order in **7H** concentration, suggesting parallel homolytic and heterolytic hydridocobaloxime pathways. Detailed mechanistic work indicated that the homolytic pathway predominates with a rate constant of $1.7 \times 10^4\ M^{-1}\ s^{-1}$. Since the hydridocobaloxime protonation rate constant was found to be $0.42\ M^{-1}\ s^{-1}$, the heterolytic pathway is competitive only at low catalyst or high acid concentrations.

Fontecave and co-workers investigated catalysis by **1** in both DMF and CH_3CN;[49] (*p*-cyanoanilinium)BF_4 was shown to give rise to irreversible cathodic waves near the $Co^{II/I}$ potential, indicative of electrocatalytic proton reduction. Lower current densities were seen near the same potential when CF_3COOH was employed as a proton source and an additional catalytic wave appeared near −1.0 V vs SCE, which was attributed to the reduction of $Co^{III}H$ to $Co^{II}H$ and subsequent reaction. With a weak acid, $[Et_3NH]Cl$, catalytic waves were observed near the $Co^{I/"0"}$ potential (−1.47 V vs SCE). Since Co^I is not sufficiently basic to be protonated by this acid and the thermodynamic potential for hydrogen evolution from $[Et_3NH]Cl$ lies negative of the $Co^{II/I}$ potential, catalysis was not seen until the second reduction. It is noted that the peak currents at these negative potentials were convoluted with direct $[Et_3NH]Cl$ reduction at the glassy carbon electrode. Modeling of the cyclic voltammetry data[67] suggested that reactions with (*p*-cyanoanilinium)BF_4 and CF_3COOH proceed by a heterolytic proton reduction (monometallic pathway) via both $Co^{III}H$ and $Co^{II}H$. It was concluded that with acids strong enough to protonate both Co^I and $Co^{III}H$ (e.g., (*p*-cyanoanilinium)BF_4), hydrogen evolution occurred via a heterolytic pathway. In cases where the acid is strong enough to protonate Co^I but not the $Co^{III}H$ intermediate, the hydride is further reduced to $Co^{II}H$ before reacting either heterolytically or homolytically. Weak acids like $[Et_3NH]Cl$ that are unable to protonate the Co^I intermediate can protonate "Co^0", and H_2 evolution can be catalyzed through the intermediacy of a $Co^{II}H$ species.

Cyclic voltammograms of **1** and **2** also showed catalytic waves upon addition of $TsOH \cdot H_2O$, as discussed above.[50] The shape of the catalytic wave of **1** indicated a rapid reaction limited by proton diffusion to the electrode surface. At higher concentrations of $TsOH \cdot H_2O$, the wave approached but did not reach a plateau. A quasi-reversible peak at about −1.0 V vs SCE observed for **1** at low acid concentration was attributed to the $Co^{III}H/Co^{II}H$ couple; the reduction potential was similar to that seen for cobalt(III) alkyl species.[68] Because catalysis at the $Co^{II/I}$ potential was relatively rapid, the concentration of $Co^{III}H$ remained low in the reaction layer near the electrode, and only small amounts of $Co^{II}H$ were generated under these conditions (the hydride reacts slowly with itself or with acid at low concentrations).

Catalytic waves for **2** reached a plateau at high concentrations of $TsOH \cdot H_2O$, indicating that catalyst reduction at the

electrode is equal to the rate of reoxidation. At lower acid concentrations, a second wave observed at −0.85 V vs SCE indicated electrocatalytic hydrogen evolution by a $Co^{II}H$ species formed by reduction of $Co^{III}H$. Because the catalytic reaction of **2** is slow compared with that of **1**, concentrations of $Co^{III}H$ and acid are high enough to yield catalytic behavior upon reduction to $Co^{II}H$.

On the basis of digital simulations of catalytic waves of **1** in the presence of $TsOH \cdot H_2O$, it was concluded that bimolecular reactivity of $Co^{III}H$ was responsible for hydrogen evolution, consistent with the findings of Chao and Espenson.[66] Catalytic waves of **2**, however, could be simulated equally well assuming either a heterolytic or homolytic mechanism thus neither reaction pathway has been identified as predominant. Because electrocatalysis occurred near the $Co^{II/I}$ reduction potentials, it was concluded that pathways through $Co^{II}H$ were unlikely, although those routes could open up at more negative potentials.

In an attempt to shed more light on H_2 evolution pathways, Peters and co-workers evaluated catalysis by **1** with (*p*-cyanoanilinium)BF_4, employing higher acid/catalyst ratios (>10) than in earlier work.[50] With ratios less than 10, these simulations were successful for both homolytic and heterolytic pathways. Over a wider range (1:1 to 40:1), however, the data could only be simulated successfully assuming a homolytic route for H_2 evolution.

The overall rate constant for H_2 evolution was estimated directly from the plateau currents. For complexes **1** and **2**, the rate constants are 7×10^3 and $\sim 2 \times 10^2$ M^{-1} s^{-1}, respectively. In both cases, the reactions are first-order in acid concentration. On the basis of these data, it is clear that hydride formation is a key step in the catalysis of H_2 evolution.

Attempts to isolate a $Co^{III}H$ complex with glyoxime ligands have been unsuccessful, except for the kinetically stabilized phosphine-supported hydride **7H**.[66] Protonation of isolable Co^{I} species with a variety of proton sources, as well as reaction of Co^{III} halide species with borohydrides, consistently yielded Co^{II} complexes and H_2, suggesting that $Co^{III}H$ is extremely reactive.[50]

Photocatalytic hydrogen generation systems are considerably more complex than the corresponding electrocatalytic ones. Reactions in photosystems with tertiary amine sacrificial donors (TEOA or Et_3N) are set out in Scheme 2. The excited photosensitizer (PS*) can be quenched by cobaloxime, producing PS^+, which reacts with $R_2N{-}CH_2{-}R'$ to generate $R_2N{-}CH_2{-}R'^+$; PS* also can be reductively quenched by $R_2N{-}CH_2{-}R'$, producing PS^-. Decomposition of $R_2N{-}CH_2{-}R'^+$ yields a proton and a second reducing equivalent, $R_2N{-}CH{-}R'$. Co^{II} can be reduced by PS*, PS^-, or $R_2N{-}CH{-}R'$ and is then protonated to give $Co^{III}H$, which can be reduced to $Co^{II}H$ by any of the powerful reductants. The weakly basic conditions under which these photocatalytic systems operate disfavor protonation of $Co^{III}H$.

SCHEME 2. H_2 Evolution Pathways in Photochemical Systems[a]

$$PS \xrightarrow{h\nu} PS^*$$

$$PS^* + Co^{II} \rightarrow PS^+ + Co^{I}$$

$$PS^+ + R_2\ddot{N}\text{-}CH_2\text{-}R' \rightarrow PS + R_2\ddot{N}\text{-}CH_2\text{-}R'^+$$

$$PS^* + R_2\ddot{N}\text{-}CH_2\text{-}R' \rightarrow PS^- + R_2\ddot{N}\text{-}CH_2\text{-}R'^+$$

$$PS^- + Co^{II} \rightarrow PS + Co^{I}$$

$$R_2\ddot{N}\text{-}CH_2\text{-}R'^+ \rightarrow H^+ + R_2\ddot{N}\text{-}CH\text{-}R'$$

$$R_2\ddot{N}\text{-}CH\text{-}R' + Co^{II} \rightarrow R_2N^+{=}CH\text{-}R' + Co^{I}$$

$$Co^{I} + H^+ \rightarrow Co^{III}H$$

$$PS^- + Co^{III}H \rightarrow PS + Co^{II}H$$

$$PS^* + Co^{III}H \rightarrow PS^+ + Co^{II}H$$

$$R_2\ddot{N}\text{-}CH\text{-}R' + Co^{III}H \rightarrow R_2N^+{=}CH\text{-}R' + Co^{II}H$$

$$R_2N^+{=}CH\text{-}R' \rightarrow \text{glycoaldehyde and di(ethanol)amine}$$

[a] The $Co^{III}H$ and $Co^{II}H$ intermediates may react via homolytic and heterolytic reaction pathways (Scheme 1) to evolve H_2. Similar pathways exist with Et_3N as a sacrificial electron donor.

Eisenberg's work on photochemical systems using Pt^{II} acetylide chromophores[58,59] and organic photosensitizers[60] with **3** (as well as other cobaloximes) showed that hydrogen evolution was first-order in catalyst concentration. The authors favor a monometallic route via $Co^{II}H$ to produce hydrogen. The $[Re(CO)_3Br(phen)]$/**1**/Et_3N/Et_3NH^+ system examined by Fontecave and co-workers also exhibited a first-order dependence on catalyst concentration, although above a certain concentration, the yield decreases, likely owing to competition for light absorption between the colored catalyst and photosensitizer.[61] In the $[Re(CO)_3Br(bpy)]$/**4**/TEOA/AcOH/DMF system studied by Alberto and co-workers, the observation of a second-order dependence on **4** in the rate of H_2 evolution (3.7 M^{-1} s^{-1}) led to the conclusion that the reaction occurred primarily via a homolytic route, although other mechanisms were not ruled out.[62] The authors noted that a heterolytic process likely would require the generation of $Co^{II}H$ as a reactive intermediate.

Thermodynamic Analysis of Reaction Pathways

Electrochemical hydrogen evolution catalyzed by **1**, **2**, and **3a** occurs near $Co^{II/I}$ potentials, where $Co^{III}H$ cannot be reduced further. Analysis of the barriers and driving forces associated with homolytic and heterolytic reaction pathways of $Co^{III}H$ suggests that the homolytic route is favored.[69]

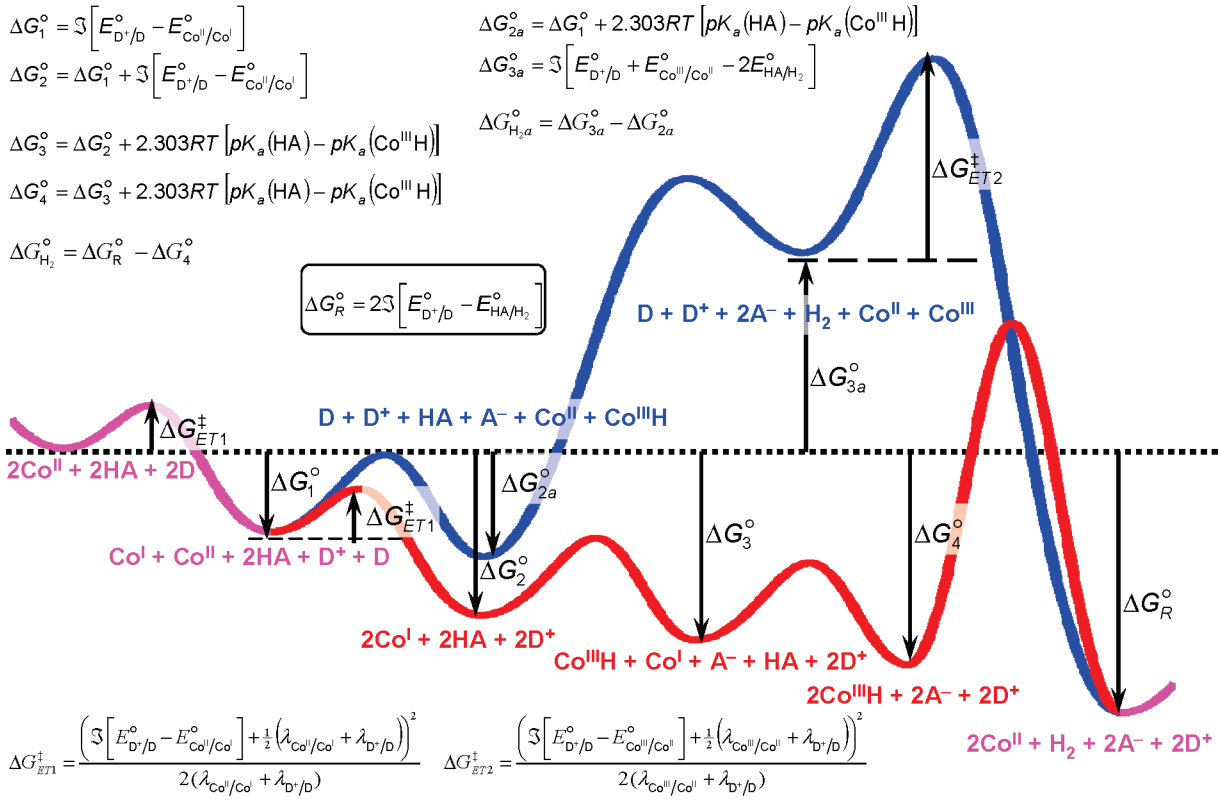

FIGURE 4. Thermodynamic analysis of cobaloxime-catalyzed H_2 evolution pathways.

As illustrated in Figure 4, the initial step in catalysis involves electron transfer from a donor (D) to Co^{II}; the barrier to this transformation ($\Delta G^\ddagger_{ET1}$) depends on the driving force and reorganization parameter (λ). A nuclear reorganization energy of 1.4 eV has been estimated for $Co^{II}-Co^{I}$ electron exchange in **2**, consistent with facile electron transfer.[69]

Protonation of the reduced catalyst is described by a driving force ($\Delta G^\circ_3 - \Delta G^\circ_2$) proportional to the p$K_a$ difference of the proton donor (HA) and $Co^{III}H$. As noted above, the $Co^{III}H$ pK_a increases as $E°[Co^{II/I}]$ decreases,[51] and substantially stronger acids are required to protonate the more easily reduced complexes. More strongly reducing Co^I intermediates produce substantially stabilized $Co^{III}H$ species upon protonation by strong acids. The extent of stabilization of the hydride will directly affect its tendency to produce H_2. Weaker Co−H bonds are correlated with low-barrier homolytic cleavage to eliminate H_2.[8] The hydridicity of the hydride, however, will facilitate reaction with a proton source in heterolytic H_2 production. The free energy of hydride transfer depends on the hydride pK_a and the $Co^{III/II}$ and $Co^{II/I}$ reduction potentials: a lower pK_a corresponds to a better hydride donor.[70]

The driving force for the overall hydrogen evolution reaction (ΔG°_R) depends on the reduction potentials of the electron donor relative to the standard potential for hydrogen evolution from HA (E°_{HA/H_2}). In a homolytic reaction pathway (red curve, Figure 4), all elementary steps on the way to proton reduction are exergonic when sufficiently powerful reductants and proton sources are used. The largest barrier to catalysis likely is associated with the elementary step that forms H_2. Little is known about the rates or barriers to bimolecular reductive elimination from metal hydrides, but it is probable that the rate of H_2 formation through this elementary step will be proportional to $k_{homo1}[Co^{III}H]^2$.

In the heterolytic route (blue curve, Figure 4), H_2 is released upon protonation of $Co^{III}H$, generating Co^{III} that must be converted to Co^{II} by the pool of reducing equivalents. The driving force for this elementary H_2 forming step, ΔG°_{3a}, depends on the average of $E°[Co^{III/II}]$ and $E°[Co^{II/I}]$ (relative to the proton reduction potential), which, in most cases, renders the heterolytic reaction pathway extremely unfavorable. While exact details are not known, the reaction barrier for this step will be greater than 11 kcal mol^{-1} for Co-diglyoxime complexes and the rate of H_2 formation will likely be proportional to $k_{hetero1}[HA][Co^{III}H]$. The exergonic conversion of Co^{III} to Co^{II} by reducing equivalents involves substantial nuclear reorganization: λ for $Co^{III}-Co^{II}$ electron exchange in **2** is estimated to be ~3.9 eV,[69] almost three times greater than that for $Co^{II}-Co^{I}$ exchange.

The heterolytic pathway to H_2 evolution catalyzed by cobaloximes involves relatively high energy barriers and unfa-

vorable driving forces. Nevertheless, it is important to remember that the dominant route to H_2 formation will depend not just on the barrier heights for elementary steps but also on the relative concentrations of HA and $Co^{III}H$. At very high acid concentrations, the heterolytic pathway becomes more favorable and can be faster even with a higher barrier height.

Summary and Prospects

Electrochemical and photochemical investigations have shed light on potential pathways of cobalt-catalyzed hydrogen evolution from solutions. Our thermodynamic analysis of these pathways has emphasized the critical role played by the barriers and driving forces of the elementary steps involved in catalytic H_2 evolution; it highlights the lower barrier of a homolytic reaction pathway. To date, however, no studies have provided detailed chemical kinetics of H_2 production nor have any key intermediates been detected.

Photochemical methods coupled with time-resolved spectroscopy offer unique opportunities to identify and monitor intermediates in the reaction cycle leading to H_2 evolution. For example, laser flash-quench methods[71−73] can be used to trigger the reduction of Co^{II} to Co^{I}, permitting optical[74] or infrared[75,76] detection of intermediates on time scales appreciably shorter than those accessible by conventional stopped-flow spectroscopy. Transient spectroscopic and kinetics measurements can offer critical insights into rate-limiting processes and the mechanism as a whole. A major challenge in this area is the development of photosensitizers and electron relays that are not inhibited by acids.[77]

The low-barrier homolytic pathway relies on the diffusion of two hydride species together in solution. A rate law with a first-order dependence on both cobalt and acid is fully consistent with electrochemical data and a first-order dependence on cobalt concentration also has been found for photochemical systems. These findings, coupled with the thermodynamic preference for a homolytic route, suggest that the limiting rate may be associated with formation of the hydride. While a bimolecular reaction of cobalt hydrides may not be rate limiting, a homolytic pathway would preclude the immobilization of catalyst on an electrode surface by preventing bimolecular diffusion pathways. Although there has been very little work on immobilizing these cobaloxime species on surfaces,[78] an efficient water splitting device[3] may require catalysts to be tethered to a photoelectrode surface.

Eliminating bimolecular diffusion by covalent linking of cobalt centers in a dinuclear catalyst could potentially enhance the rate of H_2 production. Any increase in rates of H_2 production relative to that of a mononuclear analogue could be probed via electrochemical methods. Work on Ru and Os diporphyrins indicates that cofacial orientation of metallocenters enhances H_2 evolution under certain conditions.[40,42] There have been very few reports of dinuclear cobalt species with glyoxime[79] or glyoxime-like ligands,[80] and none has demonstrated proton reduction activity. Current work in our laboratory is focused on proton reduction by covalently linked dicobalt catalysts.

We thank Xile Hu, Louise Berben, Brandi Cossairt, and Jonas Peters for discussions and their important contributions to cobaloxime chemistry. This work was supported by an NSF Center for Chemical Innovation (CCI Powering the Planet, Grants CHE-0802907 and CHE-0947829), the Arnold and Mabel Beckman Foundation, CCSER (Gordon and Betty Moore Foundation), and the BP MC² program. J.L.D. is an NSF Graduate Research Fellow.

BIOGRAPHICAL INFORMATION

Jillian L. Dempsey is a graduate student at the California Institute of Technology where she is investigating the mechanism of proton reduction by cobaloximes with Harry B. Gray and Jay R. Winkler. She received her S.B. in chemistry from the Massachusetts Institute of Technology in 2005.

Bruce S. Brunschwig studied physical chemistry at the Polytechnic Institute of NYU (Ph.D. 1972) before joining the faculty of Hofstra University in 1972. He moved to Caltech in 2004 from Brookhaven National Laboratory. He is Director of the Molecular Materials Resource Center, Member of the Beckman Institute, and a Powering the Planet NSF CCI Principal Investigator.

Jay R. Winkler studied inorganic chemistry at Caltech (Ph.D. 1984). He moved to Caltech in 1990 from Brookhaven National Laboratory. He is Director of the Beckman Institute Laser Resource Center, Member of the Beckman Institute, and a Powering the Planet NSF CCI Principal Investigator.

Harry B. Gray studied inorganic chemistry at Northwestern University (Ph.D. 1960) and the University of Copenhagen (1960−1961) before joining the chemistry faculty of Columbia University. In 1966, he moved to Caltech, where he is the Arnold O. Beckman Professor of Chemistry, Founding Director of the Beckman Institute, and Powering the Planet NSF CCI Principal Investigator.

FOOTNOTES

*To whom correspondence should be addressed. E-mail addresses: bsb@caltech.edu; winklerj@caltech.edu; hbgray@caltech.edu.

REFERENCES

1 Lewis, N. S.; Nocera, D. G. Powering the planet: Chemical challenges in solar energy utilization. *Proc. Natl. Acad. Sci U.S.A.* **2006**, *103*, 15729–15735.

2 Lewis, N. S. Powering the planet. *MRS Bull.* **2007**, *32*, 808–820.

3 Gray, H. B. Powering the planet with solar fuel. *Nat. Chem.* **2009**, *1*, 112.

4 Dempsey, J. L.; Esswein, A. E.; Manke, D. R.; Rosenthal, J.; Soper, J. D.; Nocera, D. G. Molecular chemistry of consequence to renewable energy. *Inorg. Chem.* **2005**, *44*, 6879–6892.

5 *CRC Handbook of Chemistry and Physics*, 64th ed.; Weast, R. C., Astle, M. J., Beyer, W. H., Eds.; CRC Press: Boca Raton, FL, 1983; p, D-158.

6 Eisenberg, R.; Gray, H. B. Preface on making oxygen. *Inorg. Chem.* **2008**, *47*, 1697–1699.

7 Koelle, U. Transition metal catalyzed proton reduction. *New J. Chem.* **1992**, *16*, 157–169.

8 Artero, V.; Fontecave, M. Some general principles for designing electrocatalysts with hydrogenase activity. *Coord. Chem. Rev.* **2005**, *249*, 1518–1535.

9 Britton, H. T. S. *Hydrogen Ions*, 4th ed.; Chapman & Hall: London, 1955; Vol. 1, pp 50−59.

10 Frey, M. Hydrogenases: Hydrogen-activating enzymes. *ChemBioChem* **2002**, *3*, 153–160.

11 Shima, S.; Thauer, R. K. A third type of hydrogenase catalyzing H_2 activation. *Chem. Rec.* **2007**, *7*, 37–46.

12 Adams, M. W. W. The structure and function of iron-hydrogenases. *Biochem. Biophys. Acta* **1990**, *1020*, 115–145.

13 Liu, X.; Ibrahim, S. K.; Tard, C.; Pickett, C. J. Iron-only hydrogenase: Synthetic, structural and reactivity studies of model compounds. *Coord. Chem. Rev.* **2005**, *249*, 1641–1652.

14 Capon, J.-F.; Gloaguen, F.; Schollhammer, P.; Talarmin, R. Catalysis of the electrochemical H_2 evolution by di-iron sub-site models. *Coord. Chem. Rev.* **2005**, *249*, 1664–1676.

15 Darensbourg, M. Y.; Lyon, E. J.; Smee, J. J. The bio-organometallic chemistry of active site iron in hydrogenases. *Coord. Chem. Rev.* **2000**, *206*, 533–561.

16 Liu, T.; Darensbourg, M. Y. A mixed-valent, Fe(II)Fe(I), diiron complex reproduces the unique rotated state of the [FeFe] hydrogenase active site. *J. Am. Chem. Soc.* **2007**, *129*, 7008–7009.

17 Justice, A. K.; Rauchfuss, T. B.; Wilson, S. R. Unsaturated, mixed-valence diiron dithiolate model for the H_{ox} state of the [FeFe] hydrogenase. *Angew. Chem., Int. Ed.* **2007**, *46*, 6152–6154.

18 Bouwman, E.; Reedijk, J. Structural and functional models related to the nickel hydrogenases. *Coord. Chem. Rev.* **2005**, *249*, 1555–1581.

19 Guo, Y.; Wang, H.; Xiao, Y.; Vogt, S.; Thauer, R. K.; Shima, S.; Volker, P. I.; Rauchfuss, T. B.; Pelmenschikov, V.; Case, D. A.; Alp, E. E.; Sturhahn, W.; Yoda, Y.; Cramer, S. P. Characterization of the Fe site in iron-sulfur cluster-free hydrogenase (Hmd) and of a model compound via nuclear resonance vibrational spectroscopy (NRVS). *Inorg. Chem.* **2008**, *47*, 3969–3977.

20 Wang, X.; Li, Z.; Zeng, X.; Luo, Q.; Evans, D. J.; Pickett, C. J.; Lu, X. The iron centre of the cluster-free hydrogenase (Hmd): Low-spin Fe(II) or low-spin Fe(0). *Chem. Commun.* **2008**, 3555–3557.

21 Obrist, B. V.; Chen, D.; Ahrens, A.; Schünemann, V.; Scopelliti, R.; Hu, X. An iron carbonyl pyridonate complex related to the active site of the [Fe]-hydrogenase (Hmd). *Inorg. Chem.* **2009**, *48*, 3514–3516.

22 Tye, J. W.; Hall, M. B.; Darensbourg, M. Y. Better than platinum? Fuel cells energized by enzymes. *Proc. Natl. Acad. Sci. U.S.A.* **2005**, *102*, 16911–16912.

23 Gloaguen, F.; Rauchfuss, T. B. Small molecule mimics of hydrogenases: Hydrides and redox. *Chem. Soc. Rev.* **2009**, *38*, 100–108.

24 Gray, H. B.; Malmstrom, B. G.; Williams, R. J. P. Copper coordination in blue proteins. *J. Biol. Inorg. Chem.* **2000**, *5*, 551–559.

25 Gloaguen, F.; Lawrence, J. D.; Rauchfuss, T. B. Biomimetic hydrogen evolution catalyzed by an iron carbonyl thiolate. *J. Am. Chem. Soc.* **2001**, *123*, 9476–9477.

26 Darensbourg, M. Y.; Lyon, E. J.; Zhao, X.; Georgakaki, I. P. The organometallic active site of [Fe]hydrogenase: Models and entatic states. *Proc. Natl. Acad. Sci. U.S.A.* **2003**, *100*, 3683–3688.

27 Ott, S.; Kritikos, M.; Akermark, B.; Sun, L. C.; Lomoth, R. A biomimetic pathway for hydrogen evolution from a model of the iron hydrogenase active site. *Angew. Chem., Int. Ed.* **2004**, *43*, 1006–1009.

28 Tard, C.; Liu, X.; Ibrahim, S. K.; Burschi, M.; De Gioia, L.; Davies, S. C.; Yang, X.; Wang, L.-S.; Sawers, G.; Pickett, C. J. Synthesis of the H-cluster framework of iron-only hydrogenase. *Nature* **2005**, *433*, 610–613.

29 Oudart, Y.; Artero, V.; Pecaut, J.; Fontecave, M. [Ni(xbsms)Ru$(CO)_2Cl_2$]: A bioinspired nickel−ruthenium functional model of [NiFe] hydrogenase. *Inorg. Chem.* **2006**, *45*, 4334–4336.

30 Ogo, S.; Kabe, R.; Uehara, K.; Kure, B.; Nishimura, T.; Menon, S. C.; Harada, R.; Fukuzumi, S.; Higuchi, Y.; Ohhara, T.; Tamada, T.; Kuroki, R. A dinuclear Ni(μ-H)Ru complex derived from H_2. *Science* **2007**, *316*, 585–587.

31 Olson, M. T.; Barton, B. E.; Rauchfuss, T. B. Hydrogen activation by biomimetic diiron dithiolates. *Inorg. Chem.* **2009**, *48*, 7507–7509.

32 Kellet, R. M.; Spiro, T. G. Cobalt(I) porphyrin catalysts of hydrogen production from water. *Inorg. Chem.* **1985**, *24*, 2373–2377.

33 Collin, J.-P.; Jouaiti, A.; Sauvage, J.-P. Electrocatalytic properties of Ni(cyclam)$^{2+}$ and Ni_2(biscyclam)$^{4+}$ with respect to CO_2 and H_2O reduction. *Inorg. Chem.* **1988**, *27*, 1986–1990.

34 Etros, L. L.; Thorp, H. H.; Brudvig, G. W.; Crabtree, R. H. Towards a functional model of hydrogenase: Electrocatalytic reduction of protons to dihydrogen by a nickel macrocyclic complex. *Inorg. Chem.* **1992**, *31*, 1722–1724.

35 Krishnan, C. V.; Sutin, N. Homogeneous catalysis of the photoreduction of water by visible light. 2. Mediation by a tris(2,2′-bipyridine)ruthenium(II)-cobalt(II) bipyridine system. *J. Am. Chem. Soc.* **1981**, *103*, 2141–2142.

36 Rillema, D. P.; Endicott, J. F. Catalysis of "Franck-Condon forbidden" electron-transfer reactions by macrocyclic cobalt(II) complexes. *Inorg. Chem.* **1976**, *15*, 1459–1461.

37 Abdel, Hamid, R.; El-Sagher, H. M.; Abdel-Mawgoud, A. M. Electrochemistry of the bis(1,4,7-triazacyclodecane)cobalt(III) complex and its role in the catalytic reduction of hydrogen. *Polyhedron* **1998**, *17*, 4535–4541.

38 Bernardt, P. V.; Jones, L. A. Electrochemistry of macrocyclic cobalt(III/II) hexaamines: Electrocatalytic hydrogen evolution in aqueous solution. *Inorg. Chem.* **1999**, *38*, 5086–5090.

39 Felton, G. A. N.; Glass, R. S.; Lichtenberger, D. L.; Evans, D. H. Iron-only hydrogenase mimics. Thermodynamic aspects of the use of electrochemistry to evaluate efficiency for hydrogen generation. *Inorg. Chem.* **2006**, *45*, 9181–9184.

40 Collman, J. P.; Wagenknect, P. S.; Lewis, N. S. Hydride transfer and dihydrogen elimination from osmium and ruthenium metalloporphyrin hydrides: Model processes for hydrogenase enzymes and the hydrogen electrode reaction. *J. Am. Chem. Soc.* **1992**, *114*, 5665–5673.

41 Grass, V.; Lexa, D.; Saveant, J. M. Electrochemical generation of rhodium porphyrin hydrides. Catalysis of hydrogen evolution. *J. Am. Chem. Soc.* **1997**, *119*, 7526–7532.

42 Collman, J. P.; Ha, Y. Y.; Wagenknect, P. S.; Lopez, M. A.; Guilard, R. Cofacial bisorganometallic diporphyrins: Synthetic control in proton reduction catalysis. *J. Am. Chem. Soc.* **1993**, *115*, 9080–9088.

43 Bhugun, I.; Lexa, D.; Saveant, J. M. Homogeneous catalysis of electrochemical hydrogen evolution by iron(0) porphyrins. *J. Am. Chem. Soc.* **1996**, *118*, 3982–3983.

44 Appel, A. M.; DuBois, D. L.; Rakowski DuBois, M. Molybdenum-sulfur dimers as electrocatalysts for the production of hydrogen and low overpotentials. *J. Am. Chem. Soc.* **2005**, *127*, 12717–12726.

45 Wilson, A. D.; Newell, R. H.; McNevin, M. J.; Muckerman, J. T.; DuBois, M. R.; DuBois, D. L. Hydrogen oxidation and production using nickel-based molecular catalysts with positioned proton relays. *J. Am. Chem. Soc.* **2006**, *128*, 358–366.

46 Connolly, P.; Espenson, J. H. Cobalt-catalyzed evolution of molecular hydrogen. *Inorg. Chem.* **1986**, *25*, 2684–2688.

47 Tovrog, B. S.; Kitko, D. J.; Drago, R. S. Nature of the bound oxygen in a series of cobalt dioxygen adducts. *J. Am. Chem. Soc.* **1976**, *98*, 5144–5153.

48 Hu, X.; Cossairt, B. M.; Brunschwig, B. S.; Lewis, N. S.; Peters, J. C. Electrocatalytic hydrogen evolution by cobalt difluoroboryl-diglyoximate complexes. *Chem. Commun.* **2005**, 4723–4725.

49 Baffert, C.; Artero, V.; Fontecave, M. Cobaloximes as functional models for hydrogenases. 2. Proton electroreduction catalyzed by difluoroborylbis(dimethylglyxoximato)cobalt(II) complexes in organic media. *Inorg. Chem.* **2007**, *46*, 1817–1824.

50 Hu, X.; Brunschwig, B. S.; Peters, J. C. Electrocatalytic hydrogen evolution at low overpotentials by cobalt macrocyclic glyoxime and tetraimine complexes. *J. Am. Chem. Soc.* **2007**, *129*, 8988–8998.

51 Creutz, C.; Chou, M. H.; Fujita, E.; Szalda, D. J. Reactions of hydroxymethyl and hydride complexes in water: Synthesis, structure and reactivity of a hydroxymethyl-cobalt complex. *Coord. Chem. Rev.* **2005**, *249*, 375–390.

52 Razavet, M.; Artero, V.; Fontecave, M. Proton electroreduction catalyzed by cobaloximes: Functional models for hydrogenases. *Inorg. Chem.* **2005**, *44*, 4786–4795.

53 Schrauzer, G. N.; Windgassen, R. J. Alkylcobaloximes and their relation to alkylcobalamins. *J. Am. Chem. Soc.* **1966**, *88*, 3738–3743.

54 Gray, H. B.; Maverick, A. W. Solar chemistry of metal complexes. *Science* **1981**, *214*, 1201–1204.

55 Esswein, A. J.; Nocera, D. G. Hydrogen production by molecular photocatalysis. *Chem. Rev.* **2007**, *107*, 4022–4047.

56 Hawecker, J.; Lehn, J.-M.; Ziessel, R. Efficient homogeneous photochemical hydrogen generation and water reduction mediated by cobaloxime or macrocyclic cobalt complexes. *New J. Chem.* **1983**, *7*, 271–277.

57 Wang, M.; Na, Y.; Gorlov, M.; Sun, L. Light-driven hydrogen production catalysed by transition metal complexes in homogeneous systems. *Dalton Trans.* **2009**, 6458–6467.

58 Du, P.; Knowles, K.; Eisenberg, R. A homogeneous system for the photogeneration of hydrogen from water based on a platinum(II) terpyridyl acetylide chromophore and a molecular cobalt catalyst. *J. Am. Chem. Soc.* **2008**, *130* (38), 12576–12577.

59 Du, P.; Schneider, J.; Luo, G.; Brennessel, W. W.; Eisenberg, R. Visible light-driven hydrogen production from water catalyzed by molecular cobaloxime catalysts. *Inorg. Chem.* **2009**, *48*, 4952–4962.

60 Lazarides, T.; McCormick, T.; Du, P.; Luo, G.; Lindley, B.; Eisenberg, R. Making hydrogen from water using a homogeneous system without noble metals. *J. Am. Chem. Soc.* **2009**, *131*, 9192–9194.

61 Fihri, A.; Artero, V.; Pereira, A.; Fontecave, M. Efficient H_2-producing photocatalytic systems based on cyclometalated iridium- and tricarbonylrhenium-diimine photosensitizers and cobaloxime catalysts. *Dalton Trans.* **2008**, 5567–5569.

62 Probst, B.; Kolano, C.; Hamm, P.; Alberto, R. An efficient homogeneous intermolecular rhenium-based photocatalytic system for the production of H_2. *Inorg. Chem.* **2009**, *48*, 1836–1843.

63 Fihri, A.; Artero, V.; Razavet, M.; Baffert, C.; Leibl, W.; Fontecave, M. Cobaloxime-based photocatalytic devices for hydrogen production. *Angew. Chem., Int. Ed.* **2008**, *47*, 564–567.

64 Li, C.; Wang, M.; Pan, J.; Zhang, P.; Zhang, R.; Sun, L. Photochemical hydrogen production catalyzed by polypyridyl ruthenium-cobaloxime heterobinuclear complexes with different bridges. *J. Organomet. Chem.* **2009**, *694*, 2814–2819.

65 Besora, M.; Lledó, A.; Maseras, F. Protonation of transition-metal hydrides: A not so simple process. *Chem. Soc. Rev.* **2009**, *38*, 957–966.

66 Chao, T.-H.; Espenson, J. H. Mechanism of hydrogen evolution from hydridocobaloxime. *J. Am. Chem. Soc.* **1978**, *100*, 129–133.

67 Rudolf, M. DigiElch 2.0, http://www.digielch.de/.

68 Shi, S.; Bakac, A.; Espenson, J. H. Reduction-induced cleavage of the cobalt-carbon bond in macrocyclic organocobalt complexes. *Inorg. Chem.* **1991**, *30*, 3410–3414.

69 Dempsey, J. L.; Winkler, J. R.; Gray, H. B. Kinetics of electron transfer reactions of H_2 evolving cobalt diglyoxime catalysts. *J. Am. Chem. Soc.*, submitted for publication.

70 Berning, D. E.; Noll, B. C.; DuBois, D. L. Relative hydride, proton, and hydrogen atom transfer abilities of $[HM(diphosphine)_2]PF_6$ complexes (M = Pt, Ni). *J. Am. Chem. Soc.* **1999**, *121*, 11432–11447.

71 Ogata, T.; Yanagida, S.; Brunschwig, B. S.; Fujita, E. Mechanistic and kinetic studies of cobalt macrocycles in a photochemical CO_2 reduction system: Evidence of Co-CO_2 adducts as intermediates. *J. Am. Chem. Soc.* **1995**, *117*, 6708–6716.

72 Berglund, J.; Pascher, T.; Winkler, J. R.; Gray, H. B. Photoinduced oxidation of horseradish peroxidase. *J. Am. Chem. Soc.* **1997**, *119*, 2464–2469.

73 Bjerrum, M. J.; Casimiro, D. R.; Chang, I.-J.; Di Bilio, A. J.; Gray, H. B.; Hill, M. G.; Langen, R.; Mines, G. A.; Skov, L. K.; Winkler, J. R.; Wuttke, D. S. Electron transfer in ruthenium-modified proteins. *J. Bioenerg. Biomembr.* **1995**, *27*, 295–302.

74 Na, Y.; Wang, M.; Pan, J.; Zhang, P.; Åkermark, B.; Sun, L. Visible light-driven electron transfer and hydrogen generation catalyzed by bioinspired [2Fe2S] complexes. *Inorg. Chem.* **2008**, *47*, 2805–2810.

75 Wright, J. A.; Pickett, C. J. Protonation of a subsite analogue of [FeFe]-hydrogenase: mechanism of a deceptively simple reaction revealed by time-resolved IR spectroscopy. *Chem. Commun.* **2009**, 5719–5721.

76 Shih, C.; Museth, A. K.; Abrahamsson, M.; Blanco-Rodriguez, A. M.; Di Bilio, A. J.; Sudhamsu, J.; Crane, B. R.; Ronayne, K. L.; Towrie, M.; Vlcêk, A., Jr.; Richards, J. H.; Winkler, J. R.; Gray, H. B. Tryptophan-accelerated electron flow through proteins. *Science* **2008**, *320*, 1760–1762.

77 Na, Y.; Pan, J.; Wang, M.; Sun, L. Intermolecular electron transfer from photogenerated $Ru(bpy)_3^{+}$ to [2Fe2S] model complexes of the iron-only hydrogenase active site. *Inorg. Chem.* **2007**, *46*, 3813–3815.

78 Pantani, O.; Anxolabéhère-Mallart, E.; Aukauloo, A.; Millet, P. Electroactivity of colalt and nickel glyoximes with regard to the electro-reduction of protons into molecular hydrogen in acidic media. *Electrochem. Commun.* **2007**, *9*, 54–58.

79 Bhuyan, M.; Laskar, M.; Gupta, B. D. Biphenyl-bridged dicobaloximes: Synthesis, NMR, CV, and X-ray study. *Organometallics* **2008**, *27*, 594–601.

80 Shimakoshi, H.; Koga, M.; Hisaeda, Y. Synthesis, characterization, and redox behavior of new dicobalt complexes having monoanionic imine/oxime-type ligands. *Bull. Chem. Soc. Jpn.* **2002**, *75*, 1553–1558.

81 Izutsu, K. *Acid-Base Dissociation Constants in Dipolar Aprotic Solvents*; Blackwell Scientific Publications: Oxford, U.K., 1990.

82 Pavlishchuk, V. V.; Addison, A. W. Conversion constants for redox potentials measured versus different reference electrodes in acetonitrile at 25°C. *Inorg. Chim. Acta* **2000**, *298*, 97–102.

83 Connelly, N. G.; Geiger, W. E. Chemical redox agents for organometallic chemistry. *Chem. Rev.* **1996**, *96*, 877–910.